Electronic Coherence, Vibrational Coherence, and Solvent Degrees of Freedom in the Femtosecond Spectroscopy of Mixed-Valence Metal Dimers in H_2O and D_2O

Philip J. Reid, Carlos Silva, and Paul F. Barbara*

Department of Chemistry, University of Minnesota, Minneapolis, Minnesota 55455

Laba Karki and Joseph T. Hupp

Department of Chemistry, Northwestern University, Evanston, Illinois 60208

Received: August 12, 1994; In Final Form: October 11, 1994[⊗]

We report the first <20-fs time-resolved pump−probe study on photoinduced intramolecular electron transfer in aqueous solution. The metal−metal, charge-transfer (MMCT) absorption bands of the mixed-valence compounds $(NH_3)_5Ru^{III}CNRu^{II}(CN)_5^-$ (RuRu) and $(NH_3)_5Ru^{III}CNFe^{II}(CN)_5^-$ (RuFe) are studied with sufficient time resolution to measure the back-electron-transfer (b-ET) time. In RuRu, the b-ET occurs in 85 ± 10 fs in H_2O and increases to 122 ± 20 fs in D_2O. Similar b-ET rates in these solvents are also observed for RuFe. The deuterium isotope effect is shown to originate from the solvent, demonstrating that hydrogenic solvent motions are directly coupled to the electron transfer event. The pump−probe spectroscopy on the MMCT band also provides information on the dynamics of the nuclear degrees of freedom (vibrational and solvent) that are coupled to the MMCT absorption band and the b-ET. An oscillatory vibrational response is observed and assigned to resonance impulsive stimulated Raman scattering. Analysis of these oscillations demonstrates that the average vibrational dephasing time for the observed modes is ~300 fs. The early-time behavior of the pump−probe transient absorption indicates that the optical dephasing time for MMCT compounds is extraordinarily short (<20 fs) due to strong solvent−solute coupling. Evidence for fast optical dephasing is provided by the instrument-response limited coherence coupling signal and the absence of a pump−probe signal corresponding to transient hole burning in the solvent coordinate. The combined results indicate that this fast b-ET is an electronically incoherent process; however, vibrational coherence is maintained for some of the degrees of freedom during the b-ET.

Introduction

Recent experiments on electron-transfer reactions have focused on the combined mechanistic role of vibrational and solvation dynamics.[1−7] This work has assisted in the development of classical and semiclassical theories which include both effects in predicting reaction rates.[8−19] Early studies on solvation dynamics centered on the role of diffusional solvation ($\tau_s \geq 500$ fs).[2,10,20−27] However, the importance of the faster, inertial solvent response (≤ 100 fs) on reaction dynamics has only recently received attention.[9,25,26,28−37] In particular, electron-transfer rates far exceeding the rate of diffusional solvation have been observed[38−43] and taken as evidence that inertial solvation[39,40] and/or fast vibrational motion[38−43] may be critical in certain ultrafast electron-transfer reactions. Also, electronic and vibrational coherence may persist on ultrafast time scales, potentially influencing the charge-transfer dynamics.[44−46] Interest in the role of coherence in electron-transfer processes has been motivated by recent femtosecond absorption experiments on photosynthetic reactions centers which suggest that vibrational coherence is maintained during the primary electron-transfer event.[47−50] Current interest centers on evaluating the importance of ultrafast solvent motion and coherence in electron-transfer reactions.

Mixed-valence metal dimers are an intriguing class of compounds in which to further investigate the dynamics of ultrafast electron-transfer processes.[51−54] Combined studies of the charge-transfer spectra and electron-transfer kinetics of metal-to-metal and metal-to-ligand charge transfer have offered an important test of contemporary electron-transfer theory.[39,55−60] The dynamics of the metal-to-metal charge transfer is investigated in this paper. This charge transfer is well represented by the ruthenium−ruthenium (RuRu) and ruthenium−iron (RuFe) compounds

$$(NH_3)_5Ru^{III}NCRu^{II}(CN)_5^- \underset{ET}{\overset{h\nu}{\rightleftharpoons}} (NH_3)_5Ru^{II}NCRu^{III}(CN)_5^-$$

$$(NH_3)_5Ru^{III}NCFe^{II}(CN)_5^- \underset{ET}{\overset{h\nu}{\rightleftharpoons}} (NH_3)_5Ru^{II}NCFe^{III}(CN)_5^-$$

Photoexcitation initiates the migration of an electron between the metal centers with internal conversion from the excited to the ground state resulting in the back-electron transfer (b-ET). Previous investigations in this laboratory on RuRu in water have demonstrated that the b-ET occurs in less than 100 fs; however, the time resolution of these experiments prohibited full disclosure of the reaction dynamics.[39,40] Experiments performed with similar time resolution on RuFe in H_2O and D_2O indicated that the back-electron transfer time is also <100 fs and that an isotope effect on the rate existed, although the nature of this effect could not be established.[43] The rapidity of this reaction combined with the potential importance of solvation suggests that mixed-valence metal dimers provide a unique opportunity to investigate the importance of inertial solvation dynamics and coherence in electron transfer.

In this paper, we report the results of a femtosecond pump−probe study on the electron-transfer dynamics of RuRu in water. Employing a 20-fs laser source, we have determined that the b-ET in RuRu occurs in 85 ± 10 fs and increases to 122 ± 20 fs in D_2O. The b-ET transfer rates of RuFe in H_2O and D_2O

* Author to whom correspondence should be addressed.

[⊗] Abstract published in *Advance ACS Abstracts,* February 1, 1995.

0022-3654/95/2099-2609$09.00/0

are also studied and found to occur on the same time scale as the b-ET in RuRu, and a deuterium-isotope effect is also observed. Experiments are presented which conclusively assign the deuterium isotope effect to the solvent, demonstrating that solvent hydrogenic vibrational modes are coupled to the electron transfer. An oscillatory component is observed in the data and assigned to impulsive excitation of Franck–Condon active normal modes. Analysis of the oscillatory response demonstrates that vibrational dephasing occurs in ~300 fs, indicating that the b-ET occurs before vibrational dephasing is complete. Finally, decay of the electronic coherent coupling signal within the instrument response and the absence of a transient hole-burning signal indicate that electronic dephasing is rapid (<20 fs). These results suggest that the b-ET process occurs in an electronically incoherent manner; however, vibrational coherence is maintained for at least a subset of the Raman active modes for a time scale that is significantly longer than the b-ET time.

Experimental Section

Optical excitation was provided by a Ti:sapphire oscillator based on the design of Murnane and Kapteyn.[61] The output of the laser consisted of 5-nJ, 20-fs pulses centered at 795 nm with a repetition rate of 91 MHz. A external fused-silica prism pair was employed to precompensate for broadening introduced by the spectrometer optics. The standard, interferometric-type absorption spectrometer consisted of a 90/10 beam splitter to generate the pump–probe beams. Also, a zero-order $\lambda/2$ plate combined with a calcite polarizer was placed in each beam to orient and define the polarizations. Delay of the pump pulse was controlled with a micropositioner (Newport), allowing for delays as short as 0.33 fs. The beams were focused on the sample at an 8° angle with a thin, 80-mm plano-convex singlet. The instrument response was determined by interferometric and noninterferometric cross-correlation at the sample, with both measurements providing an instrument response of 31-fs FWHM.

RuRu ($(NH_3)_5Ru^{III}CNRu^{II}(CN)_5)^-Na^+$) and RuFe($(NH_3)_5Ru^{III}CNFe^{II}(CN)_5)^-Na^+$) were synthesized by published procedures.[62] Ultrapure H_2O (Baker Laboratories) and D_2O (Cambridge Isotope Laboratories) and formamide (>99%, Fluka) were purchased and used without further purification. For the low pH experiments described below, the pH was adjusted by the addition of HCl to H_2O or of DCl to D_2O, respectively. The sample pH was measured before and after a given experiment and found to be identical to ±0.05 pH unit. Experiments at ambient temperature (20 ± 2 °C) were performed without active temperature control, whereas the temperature-dependent measurements were performed with an external temperature bath and are accurate to ±0.5 °C. The 0.3 o.d./mm sample was delivered to a 1-mm path length flowcell employing 100-μm quartz microscope cover slips as windows to minimize the contribution of glass to the observed transients. Detection was performed with matched photodiodes to monitor the intensity of the probe with and without photolysis. The diode outputs were delivered to a lock-in amplifier (Stanford Research SR850) operating in differential mode with the 2-kHz detection frequency provided by the output from a mechanical chopper placed in the pump beam path. A typical transient consisted of six to eight scans employing an 8.33 fs/step point spacing, resulting in a total acquisition time of ~2 h. Experiments with a finer point spacing were performed to ascertain the fidelity of the frequencies determined from Fourier analysis of the residuals. Data analysis consisted of fitting the transients to a sum of two exponentials convolved with the instrument response function. Finally, identical kinetics were observed for a 5-fold reduction in both pump and probe power.

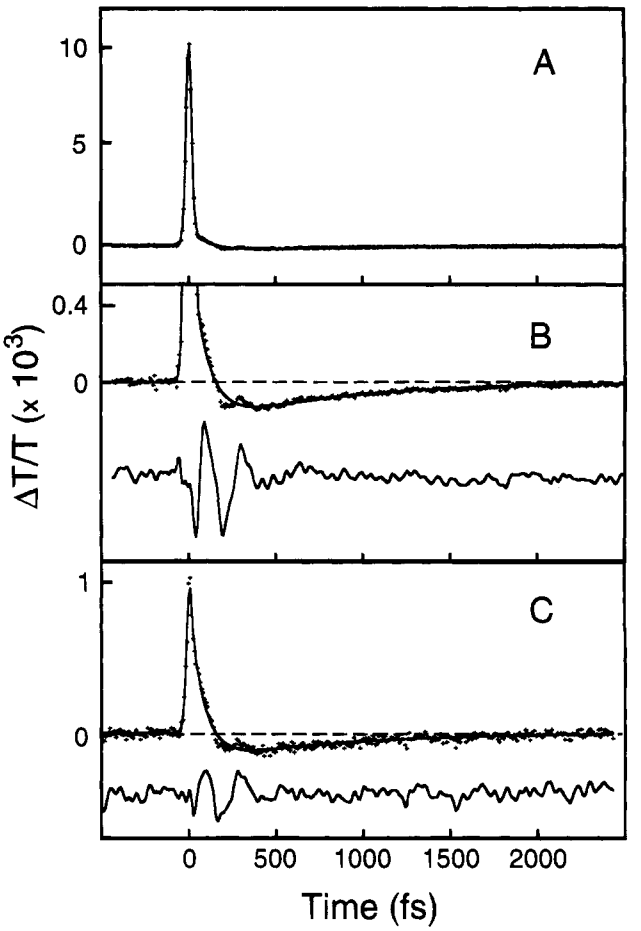

Figure 1. (A) Femtosecond absorption transient of RuRu in water obtained with pump and probe wavelengths of 795 nm. The relative orientation of the pump and probe polarizations is parallel. The solid line corresponds to the best fit of the instrument response convolved with two exponentials. (B) Expansion of A revealing the presence of the ground-state bleach and longer time absorption. Analysis of the transient resulted in a back-electron-transfer time of 85 ± 10 fs and ground-state absorption decay time of 880 ± 160 fs (Table 1). The residual difference between the fit and the data is given by the lower line, demonstrating the oscillatory response of the sample. (C) Transient obtained with perpendicular pump and probe polarizations.

Results

RuRu in H_2O and D_2O. The femtosecond absorption transient of RuRu in water is presented in Figure 1A. The transient is dominated by the symmetric signal centered at zero delay corresponding to the coherent interaction of the pump and probe beams. The origin of this type of response has been ascribed to the scattering of pump light into the probe direction via spatial modulation of the sample extinction (an amplitude grating), the sample index of refraction (phase grating), and/or degenerate four-wave mixing originating from the solvent.[63–66] The symmetric response observed here is in contrast to the asymmetry expected for a phase grating, and the absence of signal with only the solvent present suggests that the majority of the coherence signal originates from an amplitude grating. Kinetic analysis of the data established that the coherence feature follows the instrument response. In order to avoid an erroneous signal due to nonlinear optical signals from the sample cell, it

TABLE 1: Biexponential Fit Parameters for the Transient Pump–Probe Signal of RuRu ($(NH_3)_5Ru^{III}NCRu^{II}(CN)_5^-$) and RuFe ($(NH_3)_5Ru^{III}NCRu^{II}(CN)_5^-$) in Various Solvents

compd	solvent	temp, °C	τ_1, fs (A_1)[a]	τ_2, fs (A_2)
RuRu	H_2O	10	98 ± 18 (0.84)	1225 ± 140 (−0.16)
		20	85 ± 10 (0.85)	880 ± 160 (−0.15)
		33	107 ± 15 (0.81)	1004 ± 560 (−0.19)
		42	87 ± 17 (0.86)	943 ± 380 (−0.14)
		48	84 ± 10 (0.87)	1015 ± 430 (−0.13)
	D_2O	20	122 ± 20 (0.87)	800 ± 240 (−0.13)
	formamide	20	135 ± 20 (0.94)	2700 ± 1500 (0.06)
RuFe	H_2O	20	89 ± 10 (0.88)	1900 ± 1200 (0.12)
	D_2O	20	125 ± 21 (0.85)	2100 ± 1100 (0.15)

[a] Amplitudes are obtained from analysis of the transients obtained with the pump polarization orthogonal to that of the probe. The amplitudes are normalized such that $|A_1| + |A_2| = 1$. Positive and negative values indicate an increase or a decrease in transmittance, respectively.

was necessary to use especially thin (100-μm) fused silica windows and to carefully position the focus of the laser in the sample volume. Another potential error in this type of experiment arises from the high repetition rate which results in multiple excitations of the same sample volume. This effect was minimized by fast sample flowing. Furthermore, we observe no variation in the ratio of the intensity of the coherence feature to the slower kinetic components as the concentration is varied over a factor of 2 and the laser power is varied over a factor of 5. This suggests that thermal effects are not a complication in these measurements.

Closer evaluation of the transient (Figure 1B) reveals the presence of a ground-state absorption bleach that evolves into an absorption with the picosecond decay of this feature completing the dynamics. Assignment of these components is in accord with our previous analysis.[39] The bleach recovery provides a measure of the internal conversion rate, with best fit resulting in a b-ET time of 85 ± 10 fs. Since the probe central frequency is located on the red edge of the ground-state electronic transition, the transient absorption corresponds to solute vibrational excitation and/or heating of the solvent coordinate. Kinetic analysis determined that the time scale for excess energy dissipation is 880 ± 160 fs. The errors represent 1 standard deviation from the mean of 26 measurements. Also, the temperature dependence of the b-ET and ground-state solvation dynamics was investigated, with the results being presented in Table 1. Inspection of the kinetics demonstrates that the b-ET in RuRu is insensitive to changes in temperature between 10 and 48 °C. This weak temperature dependence is consistent with the b-ET occurring in the inverted regime.[1]

An oscillatory component of the kinetics is observed in the residual difference between the fit and the data (Figure 1B). The Fourier transform of the residual is presented in Figure 2A. This analysis demonstrates that the oscillations consist of multiple frequency components with large amplitudes centered at 170, 270, and 488 cm^{-1}. The latter two frequencies are in close agreement with features observed in the postresonance Raman spectrum of RuRu reported in the literature.[56,67] Recent resonance Raman experiments have demonstrated the presence of the 170-cm^{-1} component as well.[68] To estimate the ground-state vibrational dephasing time, the residual was fit to a sum of three cosine components (identical to those reported above) having separate dephasing times, resulting in an average vibrational dephasing time of ~300 fs.

To determine whether the large coherence feature obscured the determination of the slower electron transfer kinetics, absorption dichroism measurements were performed (Figure 1C). Large anisotropy values have been observed for coherence

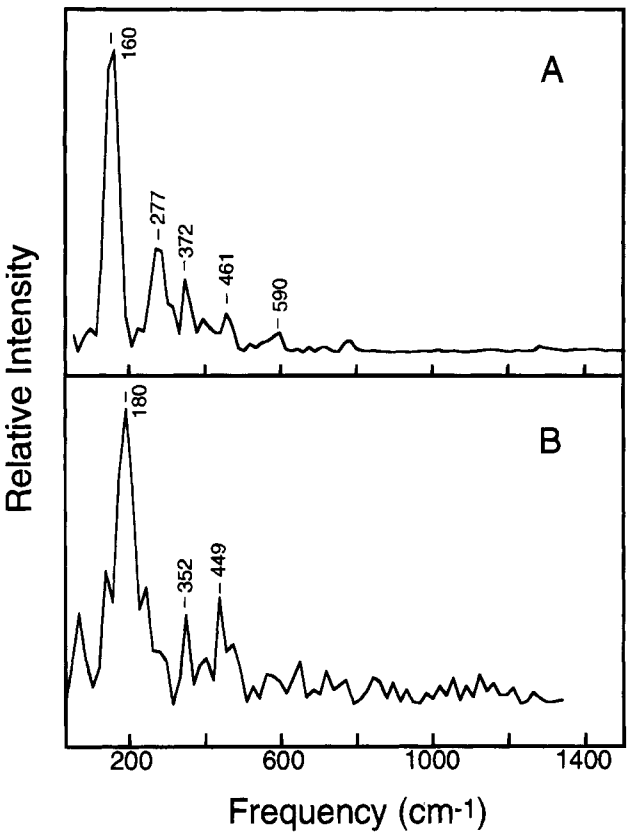

Figure 2. Fourier analysis of the residual difference between the fit and data for RuRu in H_2O (A) and formamide (B). The observed frequencies are in agreement with features observed in the postresonance Raman spectrum.[56,67,68]

signals consistent with the observed reduction in intensity of this feature with orthogonal pump and probe polarizations.[27,28] Figure 1C demonstrates that with perpendicular excitation, the amplitude of the coherence feature is dramatically reduced if not removed relative to the features corresponding to the back-electron transfer and ground-state relaxation. The anisotropy of the transient absorption signal is presented in Figure 3. The anisotropy is defined as

$$A(t,\omega) = \frac{H_{\parallel}(t,\omega) - H_{\perp}(t,\omega)}{H_{\parallel}(t,\omega) + 2H_{\perp}(t,\omega)}$$

where $H_{\parallel}$ is the signal with parallel pump and probe polarizations and $H_{\perp}$ is the signal with the pump polarization orthogonal to that of the probe. The figure demonstrates that at early times, when the coherence coupling signal is large in the parallel transient, the anisotropy approaches unity.[63,65] This large initial anisotropy decays concomitant with the coherence coupling signal to a value of 0.4 corresponding to the electron transfer and ground-state resolvation components. An anisotropy value of 0.4 is consistent with monitoring a single, dipole-allowed electronic transition before rotational reorientation.[69,70] The ability to accurately measure anisotropies was confirmed by measurements on the cyanine dye HITCI dissolved in methanol where an anisotropy of 0.4 was observed after decay of the coherence coupling signal. Finally, the kinetics observed for perpendicular excitation were in agreement with the parallel excitation results, demonstrating that we are able to effectively measure the back-electron transfer even in the presence of the coherence coupling signal.

To ascertain the role of solvent motion on the electron transfer, we performed experiments on RuRu in D_2O (Figure 4). Similar to the transient obtained in H_2O, Figure 4A

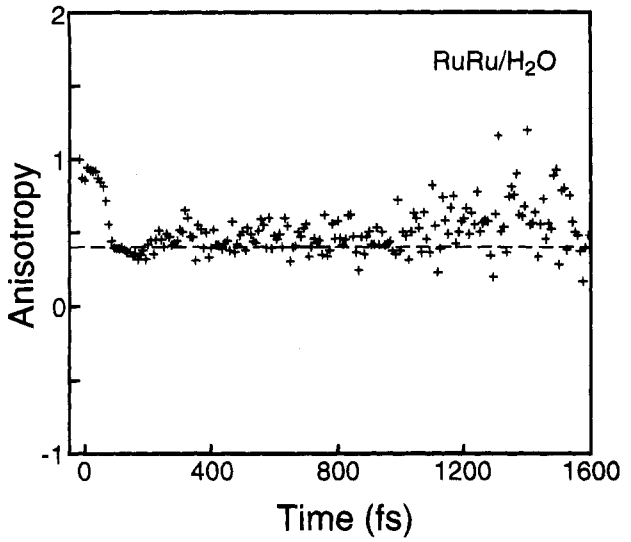

Figure 3. Temporal evolution of the absorption anisotropy for RuRu in H_2O. The anisotropy is related to the intensity observed with parallel and perpendicular probe excitation by $A(t,\omega) = (H_{||} - H_{\perp})/(H_{||} + 2H_{\perp})$, where $H_{||}$ is the signal observed with parallel pump and probe polarizations and $H_{\perp}$ is the signal where the pump polarization is orthogonal to that of the probe.

demonstrates that for parallel excitation, the dominant feature is the coherence interaction. Expansion of the transient (Figure 4B) reveals the presence of the ground-state bleach and absorption. Kinetic analysis established that coherence coupling also follows the instrument response. However, the b-ET time increases to 122 ± 20 fs. Decay of the ground-state absorption occurs in 800 ± 240 fs, similar to the time in H_2O. Similar kinetics were observed for perpendicular excitation (Figure 4C), demonstrating that the analysis of the bleach recovery is not perturbed by the presence of the large coherence signal. Finally, the residual difference between the fit and the data was Fourier analyzed and found to contain the same frequencies within experimental error (~30 cm^{-1}) to those observed in H_2O.

To address the influence of solvent/solute hydrogen exchange on the electron-transfer kinetics, the experiments were also performed at pH 2.2. The possibility exists that the back-electron-transfer rate reduction observed in D_2O reflects a decrease in frequency of accepting modes with ammine character since ammine protons are labile to exchange with the solvent. This exchange rate is roughly inversely proportional to the hydronium ion concentration.[71] Exchange at pH 2 was measured by monitoring the frequency shift of the Raman active $Ru-NH_3$ stretch from 480 to 444 cm^{-1}, corresponding to the formation of $Ru-ND_3$.[68] Measurement of the static absorption spectrum verified that protonation of the terminal CN ligands does not occur at this lower pH. This study revealed that at pH 2, the exchange half-life is 8 h, with complete exchange occurring in 24 h. Transient absorption studies were performed at 20-min intervals over a 24-h period at pH 2. No change in the bleach recovery dynamics was observed over this time, and the b-ET kinetics were determined to be 120 ± 18 fs. These kinetics are essentially identical to those observed in D_2O at pD 7. Finally, to ensure that the reduction in pH did not affect the reaction dynamics in water, the kinetics in H_2O at pH 2.2 were measured, resulting in a b-ET time of 89 ± 20 fs. This is identical to the kinetics observed at pH 7 within the error of this measurement. Therefore, the b-ET rate reduction in D_2O can be ascribed to the solvent.

RuRu in Formamide. Our pervious experiments on the b-ET of RuRu in formamide indicated that the kinetics in this solvent were also rapid; therefore, we have reinvestigated the

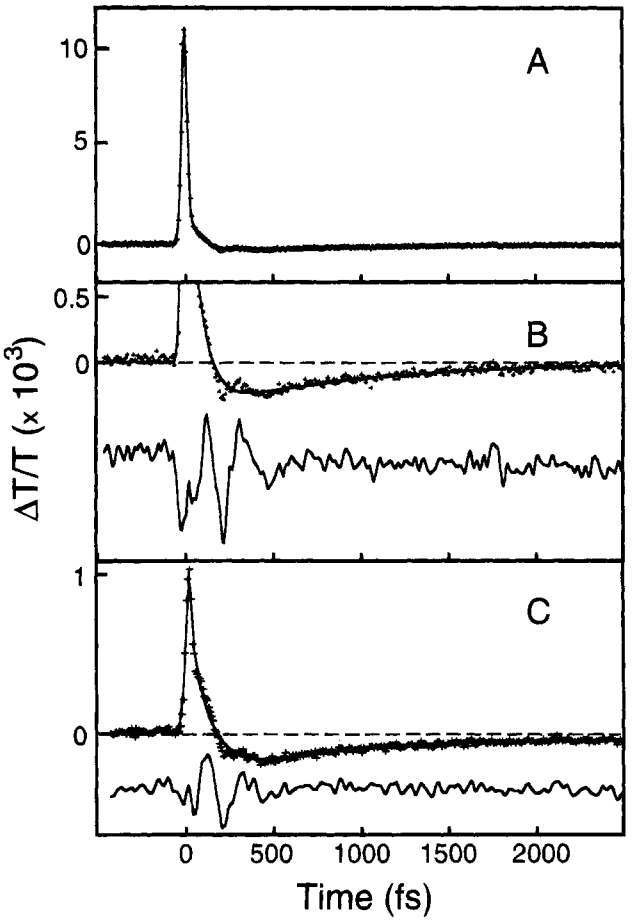

Figure 4. (A) Femtosecond absorption transient of RuRu in D_2O obtained with pump and probe wavelengths of 795 nm. The relative orientation of the pump and probe polarizations is parallel. The solid line corresponds to the best fit of the instrument response convolved with two exponentials. (B) Expansion of A revealing the presence of the ground-state bleach and longer time absorption. Analysis of the transient resulted in a back-electron transfer time of 122 ± 20 fs and ground-state absorption decay time of 800 ± 240 fs (Table 1). The residual difference between the fit and the data is given by the lower line demonstrating the oscillatory response of the sample. (C) Transient obtained with perpendicular pump and probe polarizations.

electron-transfer kinetics with the improved time resolution of the current apparatus. Figure 5 presents the observed transient with pump polarization perpendicular to that of the probe. Consistent with the results obtained on RuRu in H_2O, this polarization arrangement results in a dramatic reduction in the intensity of the coherence coupling signal, facilitating observation of the dynamics associated with the electron-transfer event. A convolution of the instrument response with a sum of two exponentials results in bleach recovery times of 135 ± 20 fs and 2.7 ± 1.5 ps. The fast component is assigned to excited-state internal conversion or the b-ET with the slower component corresponding to ground-state solvation. The MMCT absorption band of RuRu in formamide is at 771 nm, which is nearly degenerate with the laser wavelength. The amplitude of the slower bleach recovery is reduced relative to the initial bleach (Table 1) consistent with probing at the absorption maximum rather than the red edge of the MMCT absorption band.

An oscillatory component to the data is also observed in formamide similar to the results obtained in water. The bottom of Figure 5 depicts the residual difference between the data and the fit, demonstrating the presence of the oscillations. The Fourier analysis of this residual is presented in Figure 2B. Similar to the results obtained on RuRu in H_2O, major frequency components are observed at 180, 352, and 449 cm^{-1}.

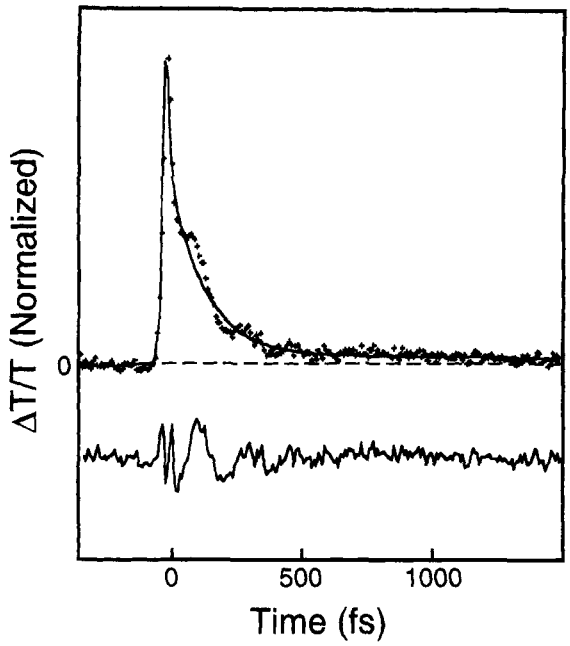

Figure 5. Femtosecond absorption transient of RuRu in formamide. The relative orientation of the pump and probe polarizations is perpendicular. The solid line corresponds to the best fit to the data by the convolution of the instrument response with the sum of two exponentials. Analysis of the transient resulted in a back-electron transfer time of 135 ± 20 fs and ground-state absorption decay time of 2.7 ± 1.5 ps (Table 1). The residual difference between the data and best fit to the data is presented in the bottom of the figure demonstrating the oscillatory response of the sample.

RuFe in H_2O and D_2O. Figure 6A presents the transient absorption observed for RuFe in H_2O. The transient was obtained with perpendicular pump and probe polarizations; therefore, the coherence coupling signal is reduced relative to the ground-state recovery and solvation dynamics (see above). A convolution of the instrument response with a sum of two exponentials resulted in a b-ET time of 89 ± 10 fs and a ground-state solvation time of 1.9 ± 1.2 ps. Since the probe is now located on the blue-edge of the MMCT absorption band (λ_{max} = 974 nm), we would expect to see a slow component of the bleach recovery corresponding to solvation of the ground-state population following internal conversion from the excited state. This is consistent with the slow component of the bleach recovery determined from the fitting and the positive amplitude of this component (Table 1). Finally, a long-lived residual bleach is observed. This feature was also observed in our previous studies on RuFe and assigned to population of excited, spin−orbit states.[39] An analysis of the transient data for RuFe in D_2O with perpendicular excitation (Figure 6B) results in a b-ET time of 125 ± 21 fs and a ground-state solvation time of 2.1 ± 1.1 ps. The magnitude of the isotope effect and b-ET kinetics for RuFe in both H_2O and D_2O are remarkably similar to the kinetics observed for RuRu.

Discussion

Solvent Kinetic Isotope Effect. The solvent deuterium isotope effect in RuRu demonstrates that hydrogenic solvent motions are coupled to the electron transfer. Molecular dynamics calculations on various charge-transfer processes in water have indicated that solvent modes with hydrogenic character corresponding to "librational" degrees of freedom are coupled to the charge-transfer event.[25,29,30,37] These broad bands fall in the frequency range of 500−900 cm^{-1} in the power spectrum of the solvent coordinate and exhibit a significant isotope effect

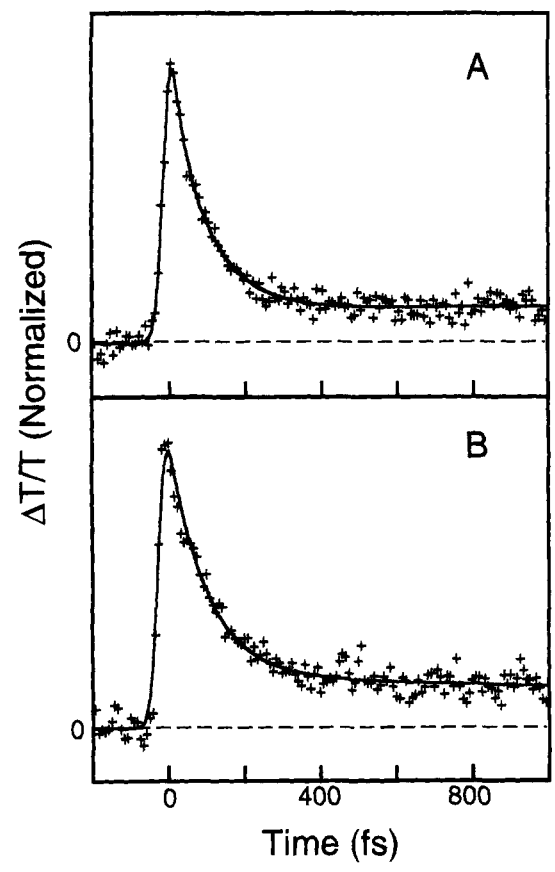

Figure 6. (A) Femtosecond absorption transient of RuFe in H_2O. The relative orientation of the pump and probe polarizations is perpendicular. The solid line corresponds to the best fit of the instrument response convolved with two exponentials. Analysis of the transient resulted in a back-electron-transfer time of 89 ± 10 fs and ground-state absorption decay time of 1.9 ± 1.2 ps (Table 1). (B) Femtosecond absorption transient of RuFe in D_2O. The relative orientation of the pump and probe polarizations is perpendicular. The solid line corresponds to the best fit of the instrument response convolved with two exponentials. Analysis of the transient resulted in a back-electron-transfer time of 125 ± 21 fs and ground-state absorption decay time of 2.1 ± 1.1 ps (Table 1).

in the frequency domain.[29] These librational modes are important components of the time domain solvation dynamics of water, especially in the initial, "inertial" response. Recent theoretical treatments of water in terms of instantaneous normal modes have discussed the relationship of the frequency and time domain representation of solute−solvent dynamics,[72,73] and in particular the importance of the librational response in the initial decay of the solvation energy. To be consistent with the terminology in the literature, we will crudely refer to the time domain manifestations of these hydrogenic degrees of freedom of the solvent coordinate as the "inertial component," where the terms "librational" or "librational modes" will be used to describe the frequency domain coordinates.

Ascertaining the existence of ultrafast solvation dynamics, especially inertial dynamics, and their importance in electron transfer has been the goal of much recent theoretical and experimental work. Molecular dynamics simulations on aqueous solvation have revealed that the majority of the solvent response corresponds to the inertial solvation component involving librational (rotational) degrees of freedom.[25,26,28,37] Furthermore, the majority of the relaxation ascribed to the inertial dynamics is localized to solvent molecules comprising the first-solvent shell. Simulations have predicted that the temporal evolution of the inertial response is best represented as Gaussian with a half-width of ~20 fs.[25,26,37] The presence

of inertial solvation dynamics in water has been recently confirmed by time-dependent Stokes-shift measurements (TDSS) in which roughly half the solvation occurs with a time constant of <50 fs, with the remainder of the dynamics corresponding to slower, diffusional solvation with time constants of 160 and 880 fs.[31,74] Interestingly, MD simulations on the ground-state relaxation dynamics of the aqueous electron observed that the inertial component demonstrates a deuterium isotope effect of 1.4, with diffusional solvation showing little effect with isotopic substitution.[37] Similar solvation dynamics have been observed for charge transfer between Fe(II) and Fe(III) centers in water.[29,30]

In terms of contemporary electron transfer theory,[1-20] isotope effects are ascribed to either zero-point energy effects on the electron-transfer activation energies or various dynamical effects which will be discussed below. It is unlikely that the isotope effect for the b-ET of RuRu and RuFe is due to an activation energy effect since the lack of a measurable temperature dependence for the b-ET indicates that the reaction is activationless (Table 1).[1]

Alternatively, it is interesting to analyze the isotope effect in terms of the usual semiclassical nonadiabatic model for electron transfer.[12,53,54,75] The usual approach is based on the assumption that the electron-transfer process is promoted by instantaneously relaxing, classical solvent degrees of freedom; i.e., dynamic solvent effects are ignored. The classical approximation for the solvent coordinate, combined with the instantaneous relaxation approximation and the nonadiabatic assumption, automatically rules out an isotope effect for the promoting mode. Since promoting modes can be ruled out, the only alternative explanation for the isotope effect is involvement of the accepting modes in the electron transfer. Thus, the isotope effect should be assigned to the quantized accepting modes which affect the kinetics via Franck–Condon factors (FCF) between the reactant and product vibronic manifolds. The FCF's modulate, in turn, the effective electronic matrix element between the reactant and product surfaces which effect the electron transfer rate. If the librational modes of the solvent are coupled to the electron transfer process, then deuterium substitution of the solvent would lower the frequencies of these accepting modes. This reduces the average FCF for barrierless vibronic channels, i.e., the channels which dominate inverted regime reactions such as the b-ET in RuRu and RuFe. In the nonadiabatic model, therefore, the solvent isotope effect would be interpreted as an accepting mode effect involving solvent librations.

An alternative explanation of the isotope effect involves the dynamic solvent effect. In particular, if the instantaneous relaxation assumption fails in the nonadiabatic model described above, the reaction rates can become a function of the solvation dynamics.[8-20] In the case of a barrierless reaction, which is probably the case for RuRu, the dynamic solvent effect leads to an electron transfer on the same time scale as solvation. However, in the reactions studied here, the observed b-ET times are ~4 times slower than the dominant solvation time, i.e. the inertial component which is predicted to have a ~20-fs solvation time.[25,26,28] The b-ET is also ~2 times slower than the experimental estimates of this solvation time.[31] The longer b-ET may be due to several factors. First, the reaction may be partially nonadiabatic, which will decrease the electron-transfer rate. Second, the b-ET process may require a combination of diffusional and inertial solvation dynamics to complete the electron transfer process. Third, the experimental estimates for the b-ET time may be in error due to other dynamical contributions to the data such as ground-state vibrational relaxation.

It seems likely that the analysis just presented for the isotope effect, which uses the terminology of traditional and approximate electron-transfer models, is far too simplistic. Indeed, the separation of vibrational modes into promoting and accepting modes is already a great simplification which may fail for the electron transfer reactions that occur on the femtosecond time scale. Other aspects of the simpler models, such as the assumption of fast vibrational relaxation and the assumed initial conditions of the solvent and vibrational coordinates, may also be inconsistent with the RuRu and RuFe examples. A detailed nonadiabatic, molecular dynamics simulation may be necessary to fully unravel the complex electronic and nuclear dynamics of the metal–metal electron-transfer reaction class. Finally, the similar rate obtained for RuRu in formamide, which has a weaker hydrogenic component to the solvation dynamics compared to water, suggests that librational motion is not the only degree of freedom coupled to the electron-transfer process.[25]

Electronic Coherence. At early delay times, interaction between the pump and probe beams creates and interrogates the electronic coherence of the sample. This is manifested as the large coherence coupling signal centered at zero delay. The amplitude and temporal behavior of the coherence signal can provide information on the time scale for optical dephasing.[76-78] This approach has recently been utilized in investigations on the electronic dephasing of the cyanine dye HITCI in ethylene glycol.[77,78] These studies revealed that some of the approximations inherent in a simple analysis of the coherence feature, such as Markovian solvent dynamics, may not be generally applicable.[76,77] In this case, evaluating electronic dephasing dynamics from the coherence coupling signal becomes complex. However, a few conclusions concerning the electronic dephasing of RuRu can be made. The coherence term rises and decays with the instrument response, indicating that the electronic coherence decays on a time scale shorter than the pulse width (<20 fs).[65] Also, studies on the ratio of the coherence and bleach amplitudes as a function of pulse width demonstrate no change in this ratio for a factor of 2 increase in temporal width. This result is in contrast to the behavior observed for systems such as HITCI in ethylene glycol in which the electronic dephasing is comparable to the pulse width. The insensitivity of the coherence signal amplitude to changes in pulse width is consistent with fast optical dephasing.[76-78] The rapidity of electronic dephasing in RuRu provides evidence for strong interaction with the solvent typical for electron-transfer electronic transitions. This is also supported by the 3700-cm^{-1} solvent reorganization energy determined from analysis of the static absorption spectrum.[39] It should be noted that a determination of the dephasing rate from this analysis is incapable of separating homogeneous and inhomogeneous effects where two- and three-pulse photon echo techniques would be useful in eliminating this ambiguity.[79,80]

Another means for separating homogeneous and inhomogeneous contributions to optical dephasing is transient hole burning.[81-87] Since the spectral width of the laser pulse (35-nm FWHM) is narrower than the spectral width of the RuRu equilibrium absorption spectrum, transient hole burning is expected if the band is inhomogeneously broadened on the time scale of the pulse temporal width.[81,84,88] The refilling of the spectral hole would correspond to a recovery component in the pump–probe transient. The excited-state lifetime (85 fs) places an upper limit to the lifetime of the hole since ground-state recovery (i.e., the b-ET) will also result in filling of the spectral hole. If a spectral hole were produced by the pump pulse, it should broaden (fill in) on several time scales due to solvation

and vibrational dynamics, but a major component of the hole recovery should be on the time scale for inertial solvation since inertial solvation dynamics dominate aqueous solvation dynamics.[25]

The pump−probe data obtained with perpendicular polarizations are the most promising data in which to observe transient hole burning because these data are not obscured by the electronic coherence coupling signal. Nevertheless, a 20-fs component to the bleach recovery is not apparent in these data (see above). Two possible explanations exist for the absence of an obvious hole-burning/hole-filling component in the bleach recovery dynamics. First, the transient hole-burning component may be beyond the signal-to-noise ratio of the present experiments. This possibility is being theoretically investigated by spectral modeling using the various static and dynamic data on RuRu.[89] Second, the transient hole-burning feature may be absent because the intrinsic (medium free) spectrum of RuRu may be much broader than the laser bandwidth. Indeed, an extremely broad spectrum is expected due to the extraordinarily intense activity in several low- and high-frequency modes for RuRu and related MMCT compounds.[39,43] The high frequency modes lead to a significant asymmetry and bandwidth, while the strongly displaced lower frequency modes, e.g. 180 cm^{-1}, substantially fill in the vibronic spectrum.

Assuming that vibronically induced optical dephasing occurs in <20 fs, this rapid optical dephasing of the MMCT transition is relevant to the mechanism of the nonadiabatic b-ET. The b-ET involves a set of initial and final Ru(III)Ru(II)/Ru(II)-Ru(III) vibrational levels different than that prepared by optical transition. Conventional electron transfer theory suggests, however, that the different sets of levels are analogous in their dynamics. With vibronically induced dephasing on the <20-fs time scale, the 85-fs b-ET of RuRu and RuFe in water should be classified as an "electronically incoherent" process, i.e., the usual situation for electron-transfer reactions.

Vibrational Dephasing. Coherent interaction of the pump and probe also creates a displaced ground-state population via resonant impulsive stimulated Raman scattering (RISRS).[90-92] The assignment of the oscillatory response to RISRS is based on the following observations. First, a Fourier transform of the oscillatory residual reveals frequency components which correspond to Franck−Condon active normal coordinates of the solute. Second, the phase of the oscillatory response is absorptive at zero delay. Since the laser is spectrally located on the red edge of the ground-state electronic absorption, we would expect a nonequilibrium ground-state population to result in red-edge absorption intensity at early times. Finally, a phase shift in the oscillations is observed in the wavelength dispersed transient consistent with the RISRS mechanism.[89] Although impulsive excitation of the low-frequency modes by rapid internal conversion is another possibility, we would expect this mechanism to produce little intensity at early times, in contrast to the observed behavior. Furthermore, impulsive excitation by an 85-fs internal conversion process would be incapable of exciting modes whose frequency is greater than 200 cm^{-1}, in opposition to the features observed in the Fourier analysis (Figure 2). Assignment of the 170 cm^{-1} component is less certain. The vibrational spectra of water reveal the presence of a mode at 175 cm^{-1} that has been assigned to dipole-induced−dipole interactions.[93-96] Impulsive excitation of this mode would be consistent with the observation that solvent motions are coupled to the electron transfer. However, similar frequency components are observed for RuRu in formamide, suggesting that the oscillatory response originates from the solute. Further resonance Raman experiments are underway to determine the origin of this frequency component.

The decay of the oscillatory response demonstrates that the average ground-state vibrational dephasing time is ~300 fs. If we project a similar dephasing time in the excited state, internal conversion to the ground state would occur before vibrational dephasing is complete. In this limit, the back-electron transfer proceeds while vibrational coherence is maintained. This result is consistent with measurements of the energy deposition into CN stretch vibrational coordinates following internal conversion.[97,98] In this work, the back-electron transfer was found to result in the population of ground-state vibrational levels along the infrared active bridging CN stretch coordinate greater than that predicted if excited-state intramolecular vibrational relaxation were complete. Although the back-electron transfer occurs in a vibrationally coherent manner, it remains to be determined if the existence of coherence affects the electron-transfer kinetics. Theoretical modeling of these kinetics with the inclusion of coherence effects would assist in determining the role of vibrational coherence on this electron-transfer reaction.

Conclusions and Summary

In this paper, we have presented the results of a femtosecond absorption study on the electron-transfer dynamics of RuRu in aqueous solution. A large (1.4) solvent deuterium isotope effect on the back-electron transfer rate was observed, demonstrating the participation of specific solvent vibrational degrees of freedom in the reaction dynamics. The presence of a deuterium isotope effect in combination with the rapidity of the back-electron transfer suggests that the inertial component of solvation is of mechanistic importance in this reaction. Also, an oscillatory response corresponding to resonant impulsive stimulated Raman scattering was observed. Analysis of the decay of these oscillations indicates that the back-electron transfer occurs before vibrational dephasing is complete. The absence of an obvious component of transient spectral hole burning and the analysis of the pump−probe induced coherence coupling signal is preliminary evidence that electronic dephasing is complete in <20 fs for the MMCT band. This result in combination with the resonance impulsive stimulated Raman scattering results demonstrates that the b-ET occurs in an electronically incoherent but vibrationally coherent manner.

Acknowledgment. We thank Margaret Murnane and Henry Kapteyn for their assistance in the construction of the Ti:sapphire oscillator. This research was supported by the NSF and the donors of the Petroleum Research Fund, administered by The American Chemical Society (P.F.B.) and the DOE (J.T.H.).

References and Notes

(1) Barbara, P. F.; Walker, G. C.; Smith, T. P. *Science* **1992**, *256*, 975.
(2) Barbara, P. F.; Jarzeba, W. *Adv. Photochem.* **1990**, *15*, 1.
(3) Maroncelli, M.; MacInnis, J.; Fleming, G. *Science* **1989**, *243*, 1674.
(4) (a) Heitele, H. Dynamical Solvent Effects on Electron Transfer Reactions. Preprint. (b) Kosower, E. M.; Huppert, D. *Annu. Rev. Phys. Chem.* **1986**, *37*, 127.
(5) For numerous examples see: *Dynamics and Mechanisms of Photoinduced Electron Transfer and Related Phenomena*; Mataga, N., Okada, T., Masuhara, H., Eds.; North-Holland: Amsterdam, 1992.
(6) Simon, J. D.; Su, S. G. *Chem. Phys.* **1991**, *152*, 143 and references therein.
(7) Weaver, M. J.; McManis, G. E. *Acc. Chem. Res.* **1990**, *23*, 294.
(8) Walker, G. C.; Akesson, E.; Johnson, A. E.; Levinger, N. E.; Barbara, P. F. *J. Phys. Chem.* **1992**, *96*, 3728.
(9) Smith, B. B.; Staib, A.; Hynes, J. T. *Chem. Phys.* **1993**, *176*, 521.
(10) Hynes, J. T. *J. Phys. Chem.* **1986**, *90*, 3701.
(11) Bixon, M.; Jortner, J. *Chem. Phys.* **1993**, *176*, 467.

(12) Jortner, J.; Bixon, M. *J. Chem. Phys.* **1988**, *88*, 167.
(13) Rips, I.; Jortner, J. *J. Chem. Phys.* **1987**, *87*, 2090.
(14) Sumi, H.; Marcus, R. A. *J. Chem. Phys.* **1986**, *84*, 4894.
(15) Sparpaglione, M.; Mukamel, S. *J. Chem. Phys.* **1988**, *88*, 3263.
(16) Calef, D. F.; Wolynes, P. G. *J. Phys. Chem.* **1983**, *87*, 3387.
(17) Zusman, L. D. *Chem. Phys.* **1980**, *49*, 295.
(18) Zusman, L. D. *Chem. Phys.* **1983**, *80*, 29.
(19) Zusman, L. D. *Chem. Phys.* **1988**, *119*, 51.
(20) Bagchi, B. *Annu. Rev. Phys. Chem.* **1989**, *40*, 115.
(21) Castner, E. W.; Bagchi, B.; Maroncelli, M.; Webb, S. P.; Ruggiero, A. J.; Fleming, G. R. *Ber. Bunsenges. Phys. Chem.* **1988**, *92*, 363.
(22) Fonseca, T. *Chem. Phys. Lett.* **1989**, *162*, 491.
(23) Grampp, G.; Harrer, W.; Hetz, G. *Ber. Bunsenges. Phys. Chem.* **1990**, *94*, 1343.
(24) Poellinger, F.; Heitele, H.; Michel-Beyerle, M. E.; Anders, C.; Futscher, M.; Staab, H. A. *Chem. Phys. Lett.* **1992**, *198*, 645.
(25) Maroncelli, M. *J. Molec. Liquids* **1993**, *57*, 1 and personal communication.
(26) Maroncelli, M.; Fleming, G. R. *J. Chem. Phys.* **1988**, *89*, 5044.
(27) Simon, J. D. *Acc. Chem. Res.* **1988**, *21*, 128.
(28) Roy, S.; Bagchi, B. *J. Chem. Phys.* **1993**, *99*, 9938.
(29) See, for example: Bader, J. S.; Kuharski, R. A.; Chandler, D. *J. Chem. Phys.* **1990**, *93*, 230.
(30) Bader, J. S.; Chandler, D. *Chem. Phys. Lett.* **1989**, *157*, 501.
(31) Jimenez, R.; Fleming, G. R.; Kumar, P. V.; Maroncelli, M. *Nature* **1994**, *369*, 471.
(32) Rosenthal, S. J.; Jimenez, R.; Fleming, G. R.; Kumar, P. V.; Maroncelli, M. *J. Molec. Liquids* **1994**, *60*, 25.
(33) Cho, M.; Rosenthal, S. J.; Scherer, N. F.; Ziegler, L. D.; Fleming, G. R. *J. Chem. Phys.* **1992**, *96*, 5033.
(34) Rosenthal, S. J.; Xie, X.; Du, M.; Fleming, G. R. *J. Chem. Phys.* **1991**, *95*, 4715.
(35) Song, X.; Marcus, R. A. *J. Chem. Phys.* **1993**, *99*, 7768.
(36) Levy, R. M.; Kitchen, D. B.; Blair, J. T.; Krogh-Jespersen, K. *J. Phys. Chem.* **1990**, *94*, 4470.
(37) Barnett, R. B.; Landman, U.; Nitzan, A. *J. Chem. Phys.* **1989**, *90*, 4413.
(38) Yoshihara, K.; Nagasawa, Y.; Yartsev, A.; Kumazaki, S.; Kandori, H.; Johnson, A. E.; Tominaga, K. *J. Photochem. Photobiol. A: Chem.* **1994**, *80*, 169.
(39) Tominaga, K.; Kliner, D. A. V.; Johnson, A. E.; Levinger, N. E.; Barbara, P. F. *J. Chem. Phys.* **1993**, *98*, 1228.
(40) Kliner, D. A. V.; Tominaga, K.; Walker, G. C.; Barbara, P. F. *J. Am. Chem. Soc.* **1992**, *114*, 8323.
(41) Tominaga, K.; Walker, G. C.; Jarzeba, W.; Barbara, P. F. *J. Phys. Chem.* **1991**, *95*, 10475.
(42) Tominaga, K.; Walker, G. C.; Kang, T. J.; Barbara, P. F.; Fonseca, T. *J. Phys. Chem.* **1991**, *95*, 10485.
(43) Walker, G. C.; Barbara, P. F.; Doorn, S. K.; Dong, Y.; Hupp, J. T. *J. Phys. Chem.* **1991**, *95*, 5712.
(44) Jean, J. M.; Fleming, G. R.; Friesner, R. A. *Ber. Bunsenges. Phys. Chem.* **1991**, *95*, 253.
(45) Jean, J. M.; Friesner, R. A.; Fleming, G. R. *J. Chem. Phys.* **1992**, *96*, 5827.
(46) Alden, R. G.; Cheng, W. D.; Lin, S. H. *Chem. Phys. Lett.* **1992**, *194*, 318.
(47) Vos, M. H.; Jones, M. R.; Hunter, C. N.; Breton, J.; Lambry, J.-C.; Martin, J.-L. *Biochemistry* **1994**, *33*, 6750.
(48) Vos, M. H.; Rappaport, F.; Lambry, J.-C.; Breton, J.; Martin, J.-L. *Nature* **1993**, *363*, 320.
(49) Martin, J.-L.; Vos, M. H. *Annu. Rev. Biophys. Biomol. Struc.* **1992**, *21*, 199.
(50) Vos, M. H.; Lambry, J.-C.; Robles, S. J.; Youvan, D. C.; Breton, J.; Martin, J.-L. *Proc. Natl. Acad. Sci. U.S.A.* **1992**, *89*, 613.
(51) Creutz, C. *Prog. Inorg. Chem.* **1983**, *30*, 1.
(52) Hush, N. S. *Prog. Inorg. Chem.* **1967**, *8*, 391.
(53) Newton, M. D.; Sutin, N. *Annu. Rev. Phys. Chem.* **1984**, *35*, 437.
(54) Ulstrup, J. *Charge Transfer Processes in Condensed Media*; Springer: Berlin, 1979.
(55) Endicott, J. F.; Song, X.; Watzky, M. A.; Buranda, T.; Lei, Y. *Chem. Phys.* **1993**, *176*, 427.
(56) Doorn, S. K.; Blackbourn, R. L.; Johnson, C. S.; Hupp, J. T. *Electrochim. Acta* **1991**, *36*, 1775.
(57) Goldsby, D. A.; Meyer, T. J. *Inorg. Chem.* **1984**, *23*, 3002.
(58) Powers, M. J.; Meyer, T. J. *J. Am. Chem. Soc.* **1980**, *102*, 1289.
(59) Meyer, T. J. *Chem. Phys. Lett.* **1979**, *64*, 417.
(60) Myers, A. B. *Chem. Phys.* **1994**, *180*, 215.
(61) Asaki, M. T.; Huang, C.-P.; Garvey, D.; Zhou, J.; Murnane, M. M.; Kapteyn, H. C. *Opt. Lett.* **1993**, *18*, 977.
(62) Vogler, A.; Osman, A. H.; Kunkely, H. *Inorg. Chem.* **1987**, *26*, 2337.
(63) Vardeny, Z.; Tauc, J. *Opt. Commun.* **1981**, *39*, 396.
(64) Eichler, H. J.; Langhans, D.; Massmann, F. *Opt. Commun.* **1984**, *50*, 117.
(65) Weiner, A. M.; Ippen, E. P. *Chem. Phys. Lett.* **1985**, *114*, 456.
(66) Palfrey, S. L.; Heinz, T. F. *J. Opt. Soc. Am. B.* **1985**, *2*, 674.
(67) Doorn, S. K.; Hupp, J. T. *J. Am. Chem. Soc.* **1989**, *111*, 1142.
(68) Petrov, V. Unpublished results, 1994
(69) Hochstrasser, R. M.; Pereira, M. A.; Share, P. E.; Sarisky, M. J.; Kim, Y. R.; Repinec, S. T.; Sension, R. J.; Thorne, J. R. G.; Iannone, M.; Diller, R.; Anfinrud, P. A.; Han, C.; Lian, T.; Locke, B. *Proc. Indian Acad. Sci. (Chem. Sci.)* **1991**, *103*, 351.
(70) Szabo, A. *J. Chem. Phys.* **1984**, *81*, 150.
(71) House, D. A. *Coord. Chem. Rev.* **1992**, *114*, 456.
(72) (a) Cho, M.; Fleming, G. R.; Saito, S.; Ohmine, I.; Stratt, R. M. *J. Chem. Phys.* **1994**, *100*, 6672. (b) Stratt, R. M.; Cho, M. *J. Chem. Phys.* **1994**, *100*, 6700.
(73) Ohmine, I.; Tanaka, H. *Chem. Rev.* **1993**, *93*, 2545.
(74) Jarzeba, W.; Walker, G. C.; Johnson, A. E.; Kahlow, M. A.; Barbara, P. F. *J. Phys. Chem.* **1988**, *92*, 7039.
(75) (a) Efrima, S.; Bixon, M. *Chem. Phys. Lett.* **1974**, *25*, 34. (b) Efrima, S.; Bixon, M. *Chem. Phys.* **1976**, *13*, 447.
(76) Balk, M. W.; Fleming, G. R. *J. Chem. Phys.* **1986**, *83*, 4300.
(77) Cong, P.; Yan, Y. J.; Deuel, H. P.; Simon, J. D. *J. Chem. Phys.* **1994**, *100*, 7855.
(78) Cong, P.; Deuel, H. P.; Simon, J. D. *Chem. Phys. Lett.* **1993**, *212*, 367.
(79) Bigot, J.-Y.; Portella, M. T.; Schoenlein, R. W.; Bardeen, C. J.; Migus, A.; Shank, C. V. *Phys. Rev. Lett.* **1991**, *66*, 1138.
(80) Nibbering, E. T. J.; Wiersma, D. A.; Duppen, K. *Phys. Rev. Lett.* **1991**, *66*, 2464.
(81) Kang, T. J.; Yu, J.; Berg, M. *J. Chem. Phys.* **1991**, *94*, 2413.
(82) Kang, T. J.; Yu, J.; Berg, M. *Chem. Phys. Lett.* **1990**, *174*, 476.
(83) Littau, K. A.; Dugan, M. A.; Chen, S.; Fayer, M. D. *J. Chem. Phys.* **1992**, *96*, 3484.
(84) Kinoshita, S.; Itoh, H.; Murakami, H.; Mitasaka, H.; Okada, T.; Mataga, N. *Chem. Phys. Lett.* **1990**, *166*, 123.
(85) Pollard, W. T.; Frangnito, H. L.; Bigot, J.-Y.; Shank, C. V.; Mathies, R. A. *Chem. Phys. Lett.* **1990**, *168*, 239.
(86) Fragnito, H. L.; Bigot, J.-Y.; Becker, P. C.; Shank, C. V. *Chem. Phys. Lett.* **1989**, *160*, 101.
(87) Brito Cruz, C. H.; Fork, R. L.; Knox, W. H.; Shank, C. V. *Chem. Phys. Lett.* **1986**, *132*, 341.
(88) Loring, R. F.; Yan, Y. J.; Mukamel, S. *J. Chem. Phys.* **1987**, *87*, 5840.
(89) Reid, P. J.; Silva, C.; Barbara, P. F. Manuscript in preparation.
(90) Walsh, A. M.; Loring, R. F. *Chem. Phys. Lett.* **1989**, *160*, 299.
(91) Banin, U.; Kosloff, R.; Ruhman, S. *Chem. Phys.* **1994**, *183*, 289.
(92) Pollard, W. T.; Dexheimer, S. L.; Wang, Q.; Peteanu, L. A.; Shank, C. V.; Mathies, R. A. *J. Phys. Chem.* **1992**, *96*, 6147.
(93) Guillot, B. *J. Chem. Phys.* **1991**, *95*, 1543.
(94) Benassi, P.; Mazzacurati, V.; Nardone, M.; Ricci, M. A.; Ruocco, G.; DeSantis, A.; Frattini, R.; Sampoli, M. *Molec. Phys.* **1987**, *62*, 1467.
(95) Walrafen, G. E. *J. Phys. Chem.* **1990**, *94*, 2237.
(96) Walrafen, G. E.; Fisher, M. R.; Hokmabadi, M. S.; Yang, W.-H. *J. Chem. Phys.* **1986**, *85*, 6970.
(97) Doorn, S. K.; Dyer, R. B.; Stoutland, P. O.; Woodruff, W. H. *J. Am. Chem. Soc.* **1993**, *115*, 6398.
(98) Doorn, S. K.; Stoutland, P. O.; Dyer, R. B.; Woodruff, W. H. *J. Am. Chem. Soc.* **1992**, *114*, 3133.

JP9421601